Molecular Switches

DOI: 10.1002/ange.201208210

Toward Functional Molecular Devices Based on Graphene–Molecule Junctions**

*Yang Cao, Shaohua Dong, Song Liu, Zhongfan Liu, and Xuefeng Guo**

Motivated by an interest in fundamental science and practical applications, researchers in molecular electronics have instigated rapid growth in this field over the past decade.[1] Different approaches have been developed to form single-molecule or ensemble molecular transport junctions (MTJs), including ones based on nanogaps fabricated by shadow mask evaporation, mechanical break junction techniques, scanning probe techniques, electroplating, lithographic methods, and electromigration,[2] and other approaches based on nanopores, mercury-drop contacts, crossbar nanostructures, and template-prepared nanowires.[3] One unique feature of these junctions is that they consist of one or a small collection of molecules as conductive elements. This implies their great potential for applications in building ultrasensitive functional optoelectronic devices[1,4] and new classes of chemo/biosensors with single-molecule sensitivity.[5] However, the ability to control the conductance of molecules through external stimuli, which is of crucial importance to the realization of practical molecular electronic devices, still challenges the field of molecular electronics.[1] So far, only a few attempts have been made to investigate the conductance switching of molecules between different states of conjugation in response to external triggers.[6] In addition, most of the previous work relies primarily on the ex situ synthesis of molecular wires (e.g., dithiolated molecules) which are subsequently inserted into the nanogapped electrodes,[2,3] thus complicating the systems because of the strong tendency of these molecules to undergo oxidative oligomerization and aggregation.[7,8] These problems could be circumvented by developing another efficient chemical way that avoids the use of dithiolated molecules and realizes the in situ synthesis of molecular wires to bridge nanogaps. In the present work, therefore, we have accomplished two tasks: 1) We have achieved the reversible conductance switching of individual azobenzene units when they are toggled back and forth between two distinct conductive states upon exposure to different external stimuli, such as light and pH; 2) We have achieved the in situ construction of complex molecular wires through the implementation of a multiple-step reaction sequence (amide formation and coordination reaction) between molecular-scale graphene point contacts.

Azobenzene, a typical photochromic molecule, can undergo reversible transitions between its *trans* and *cis* conformations when exposed to light irradiation (Figure 1 a).[9] The *trans* isomer is nearly planar, but the *cis* isomer adopts a bent conformation with its phenyl rings twisted roughly 55° relative to each other. Theoretical studies[10] suggest that this transformation yields a change in the dipole moment from near zero (*trans*) to 3 Debye (*cis*); the *trans* isomer is about 0.2 eV lower in energy and it also displays the smaller energy gap (1.98 eV) between the highest occupied molecular orbital (HOMO) and the lowest unoccupied molecular orbital (LUMO). These properties form the basis of a light-driven molecular switch.[9,11] Therefore, it is crucial to clarify the electrical transport characteristics of this molecule at the molecular level. In this work, for the first time we experimentally studied charge transport in a system where a single azobenzene unit is covalently linked to two graphene

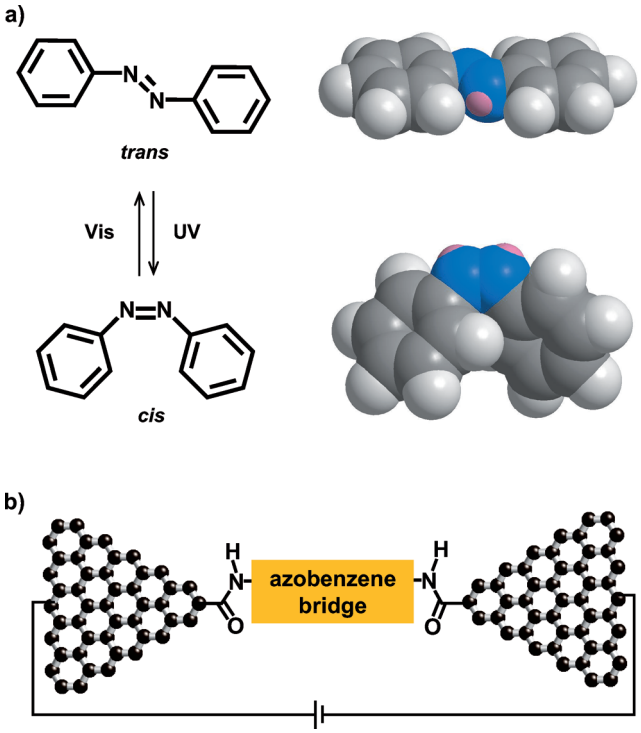

Figure 1. a) Structures and space-filling models of *trans* and *cis* isomers of azobenzene. b) Schematic representation of a graphene–azobenzene junctions.

[*] Y. Cao, S. Dong, S. Liu, Prof. Z. Liu, Prof. X. Guo
Center for NanoChemistry, Beijing National Laboratory for Molecular Sciences, State Key Laboratory for Structural Chemistry of Unstable and Stable Species
College of Chemistry and Molecular Engineering
Peking University, Beijing 100871 (P.R. China)
E-mail: guoxf@pku.edu.cn

[**] We acknowledge primary financial support from MOST (2012CB921404) and NSFC (21225311 and 51121091).

Supporting information for this article is available on the WWW under http://dx.doi.org/10.1002/anie.201208210.

point contacts (Figure 1b). An import advantage of graphene, which we chose as the electrode material, is that it is a zero-gap semiconductor that does not have the inherently variable diameter and chirality of single-walled carbon nanotubes (SWNTs). This should rule out the possibility of modulating the junction conductance by the electrode chirality as has happened in previous cases.[2i,10a]

The graphene–azobenzene devices were fabricated by a new dash-line lithographic (DLL) method described in detail elsewhere.[12] The key feature of this technique is the ability to produce carboxylic acid terminated graphene point contact arrays with gaps of at most 10 nm. In brief, we designed a DesignCAD file with a 5 nm wide dash line to open an indented window in a spin-cast layer of polymethylmethacrylate (PMMA) by using ultrahigh-resolution electron-beam lithography. The graphene sheet was then locally cut through the open window by oxygen plasma ion etching. By exploiting the gradual etching and undercutting of PMMA, we achieved narrow gaps between indented graphene point contacts. These point contacts react with conductive molecules derivatized with amino groups to form molecular devices in high yields. Furthermore, the contacts made by covalent amide bond formation are robust and thus can tolerate a broad range of chemical treatments. In conjunction with the unique properties of graphene electrodes, the ease of device fabrication and the device stability place graphene–molecule junctions as a new-generation testbed for molecular electronics.

Figure 2a shows the structure of the azobenzene unit used. Under optimized conditions, the maximum connection yield for this bridge was found to be 50%, which corresponded to a cutting yield of about 28%.[12] On the basis of these data, the analysis of the number of junctions that contribute to charge transport using the binomial distribution demonstrates that in most cases, only one or two junctions contribute to charge transport of the devices.[12] Figure 2b shows the *I*–*V* curves of a representative azobenzene-reconnected device before cutting, after cutting by means of oxygen plasma ion etching, and after further molecular connection. The black curve shows the source-to-drain (S-D) current (I_{SD}) plotted against the gate voltage (V_G) at constant S-D bias voltage ($V_{SD} = -1$ mV) before cutting. The red curve, recorded after cutting, shows no conductance down to the noise limit of the measurement (≤ 100 fA) owing to the nanogaps. After molecular connection, we observed the recovery of the original property, albeit at reduced current values (blue trace in Figure 2b). These observations are consistent with our previous studies.[12] In the following, we detail the switching and sensing functions of these graphene–azobenzene junctions.

We first studied how the reconnected devices with the azobenzene bridges responded to external stimuli such as changes in light. Figure 2c shows the typical responses for a representative rejoined device (25 working devices were examined) upon sequential irradiation with UV and visible light. As predicted theoretically,[10a] the azobenzene unit undergoes the conformational change from the *trans* form to the *cis* form under UV irradiation (254 nm) and becomes less conductive (red curve in Figure 2c). This is because the *cis*

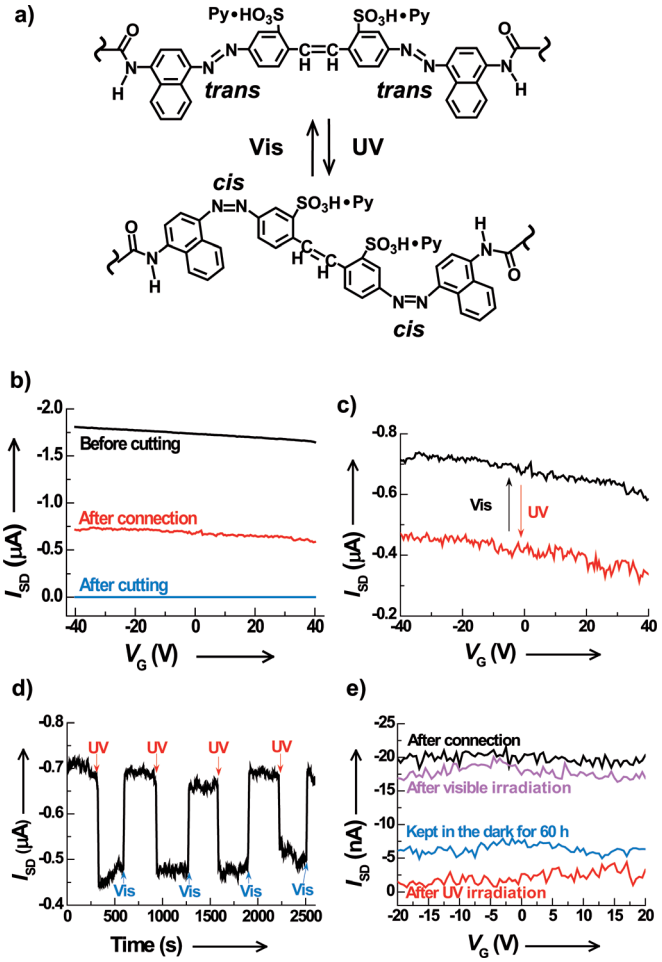

Figure 2. Photoswitching properties of devices rejoined by azobenzene molecules. a) Schematic representation of the switching mechanism for the molecule responding to UV and visible light. b) Characteristics of a representative device reconnected with the azobenzene bridge before cutting (black curve, $V_{SD} = -1$ mV), after cutting (red curve, $V_{SD} = -50$ mV), and after connection (blue curve, $V_{SD} = -50$ mV). c) Characteristics of the same device under UV- ($\lambda = 254$ nm) and visible-light irradiation ($\lambda > 460$ nm). $V_{SD} = -50$ mV. d) Time trace of the drain current for the same device showing the reversible photoswitching events under irradiation with UV light and visible light. $V_{SD} = -50$ mV; $V_G = 0$ V. e) Characteristics of another reconnected device after connection (black curve), after UV irradiation (red curve), kept in the dark for 60 h (blue curve) and after further irradiation with visible light (magenta curve). $V_{SD} = -50$ mV.

form has a larger HOMO–LUMO energy gap and/or poorer energy-level alignment with the Fermi energy in the leads. The reverse photoisomerization can be affected with visible light and thus the conductance nearly recovered to the original value (black curve in Figure 2c). To rule out potential artifacts, we carried out a series of control experiments using the devices rejoined by a unit lacking the photochromic azo groups, and the uncut and partially cut graphene FETs treated with a solution of the azobenzene derivative. None of the devices showed photoswitching properties under the same conditions (more details can be found in the Supporting Information, Figures S1–S4). To check the switching stability and reversibility, we also performed a series of UV- and

visible-light irradiations while monitoring the current changes in real time at constant V_{SD} and V_G biases for the same device. Over many switching cycles (Figure 2d), remarkably, the devices still showed stable switching between two distinct conductive states in a reversible manner. In related previous reports only one-way photoswitching was observed (using individual diarylethenes spanning either gold or SWNT electrodes[6a,e]); here we disclose the first example of a reversible light-driven single-molecule switch. In some case when the device was rejoined by multiple azobenzene bridges, we kept the reconnected devices in the dark after UV irradiation for tens of hours, and after that time these devices only showed the small conductance recovery due to the slow thermally driven back-transformation (Figure 2e). Note that the reconnected devices are light-sensitive and the difficulty of precisely controlling the light intensity hampers our investigation of the stepwise switching dynamics of individual azo groups.

In addition to photoswitching effects, another significant feature of our azobenzene linker is its sensitivity to pH (Figure 3). We expected that, owing to the presence of two sulfonic acid groups, this molecule could reversibly react with base and acid and thus become pH sensitive (Figure 3a). At the initial state after connection, the sulfonic acid groups formed pyridinium salts and showed moderate conductivity (black curve in Figure 3b). We then carried out several cycles of protonations (pH 1) and deprotonations (pH 12) while monitoring the current changes at saturation for devices that were rinsed, dried, and tested. We found that the molecular conductance changed by more than two orders of magnitude (from about $3.11\times10^{-2}\,e^2h^{-1}$ at low pH to about $1.54\times10^{-4}\,e^2h^{-1}$ at high pH) for several switching cycles (Figure 3b,c). These results are consistent with our previous observations, where protonated oligoanilines bridging SWNT point contacts showed higher conductivity than the deprotonated forms.[2i,13] Therefore, these devices provide an ultrasensitive local probe for monitoring pH based on one or a small collection of molecules. Control experiments using either the devices reconnected by a molecule lacking the pH-active groups, and the uncut and partially cut graphene FETs treated with a solution of the azobenzene derivative were performed under the same conditions. None of the devices showed the sensing effects during protonation/deprotonation (Figures S5–S7 in the Supporting Information). In combination with the switching property of the azobenzene molecule described above, these indicate an approach to integrate multiple functionalities into single-molecule devices through smart molecular designs for the construction of logic gates or even molecular computers.

After having understood the switching properties of the azobenzene molecule, we turned our attention to circumventing the previously mentioned problems associated with the oxidative oligomerization and molecular aggregation of dithiolated molecules in device fabrication and measurement using graphene–molecule junctions. To do this, we developed an efficient method for the in situ construction of molecular transport junctions by combining self-assembly and programmed chemical reactions. The two-step strategy used in this study is shown in Figure 4a. First we primed the graphene

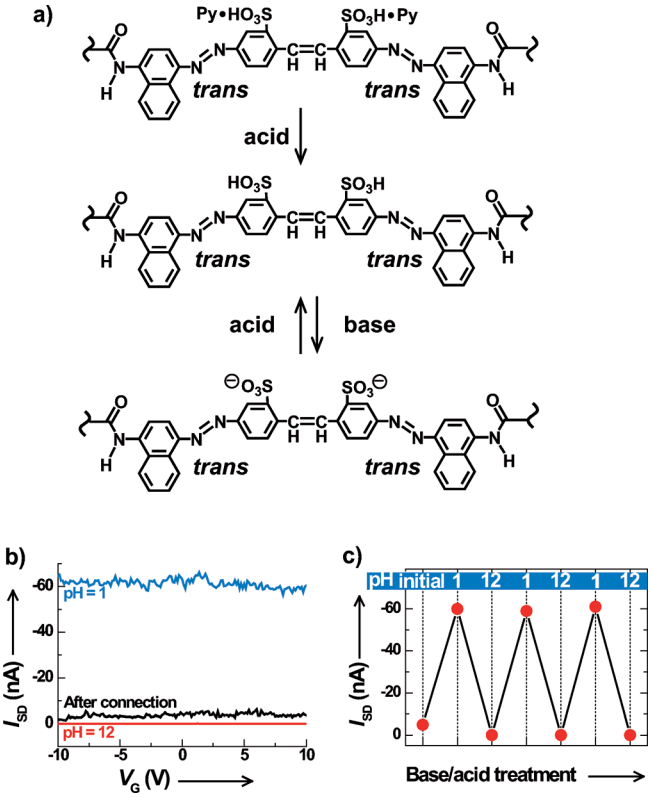

Figure 3. Sensing properties of devices rejoined by azobenzene units. a) Schematic representation of the sensing mechanism for response of the bridge to a change in pH. b) Characteristics of a device reconnected by the bridge at low pH (pH 1) and at high pH (pH 12). $V_{SD}=-50$ mV. c) Switching cycles of the conductance of the same device when alternatively immersed in solutions of low and high pH. $V_{SD}=-50$ mV; $V_G=0$ V.

point contacts with the terpyridyl ligand **1**, which has only a single amino group to react with the graphene electrodes but does have the tridentate aromatic pocket available for the subsequent coordination chemistry (Figure 4b). There was essentially no detectable current ($\leq$100 fA) after reaction with **1** using the fresh lithographically cut devices (red curve in Figure 4c). Then we immersed these primed devices in a diluted methanol solution of cobalt acetate (ca. 10^{-5} M). In this step some devices were connected through metal ion coordination and thus they became conductive (blue curve in Figure 4c). Under optimized conditions, the yield of the working devices was approximately 21% (21 out of 102 devices tested) for the two-step connection reaction.

Multistep reactions can also be carried out within the nanogaps in a stepwise approach (Figure 4a). After the second step of cobalt ion treatment, we carefully screened the *I*–*V* characteristics of the devices and determined each as either reconnected or open. The circuits that were open showed no conductance down to the noise limit of the measurement ($\leq$100 fA) (red curves in Figure 4d). Each of these devices should contain two cobalt ions, one on each facing end of the nanogap, and each cobalt ion should be available for further coordination. In the third step of this sequence the hexapyridyl **2** (Figure 4b) was added (ca. 10^{-5} M

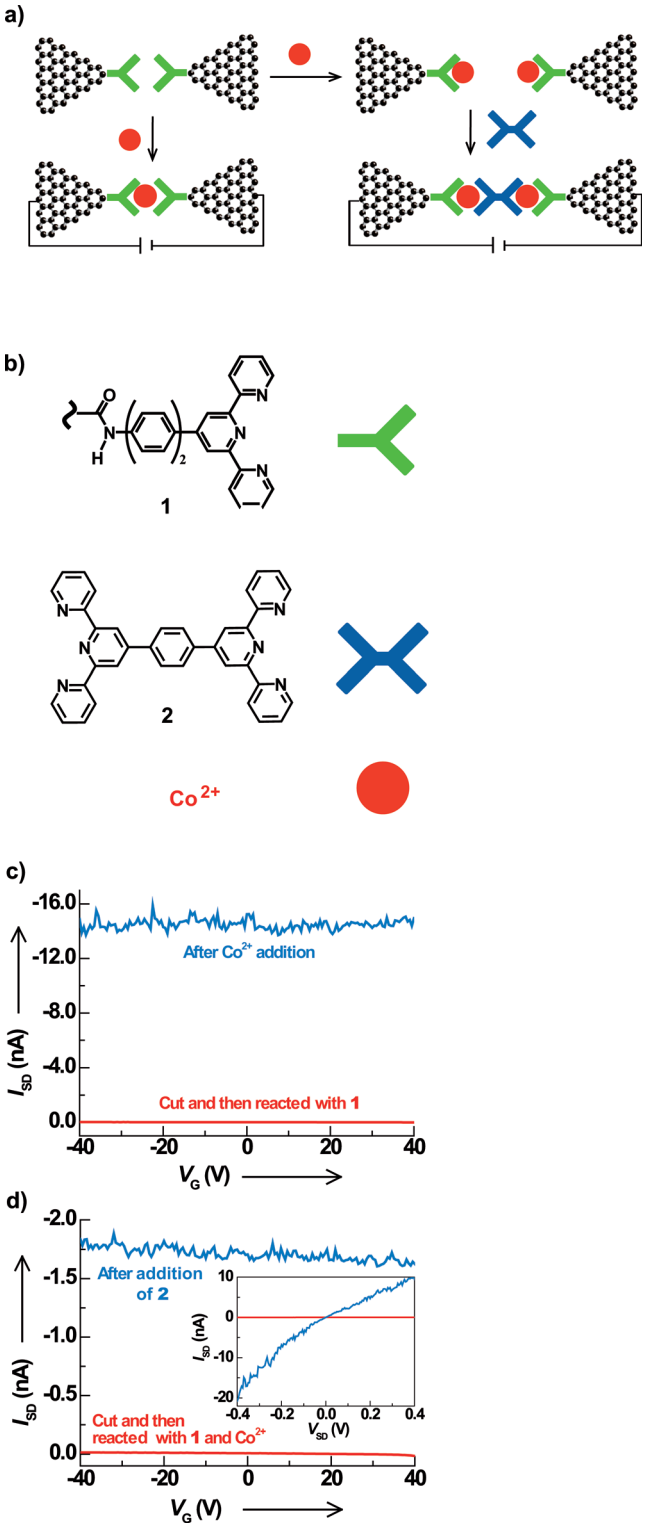

Figure 4. In situ construction of molecular junctions. a) Schematic description of strategies for bridging graphene point contacts through two-step or three-step sequences. b) Molecules used for reconnection. c) I_{SD} versus V_G plot of a device reconnected through the two-step strategy. $V_{SD} = -50$ mV. d) Device characteristics for a device reconnected through the three-step sequence. $V_{SD} = -50$ mV. Inset shows the I_{SD} versus V_{SD} plot for the same device after reactions with **1** and cobalt ions (red), and after the addition of **2** (blue) at zero gate bias.

in chloroform), and the conductivity of these devices was measured (blue curve in Figure 4d). The inset in Figure 4d shows I_{SD} as a function of V_{SD} for the same device after sequential reactions with **1** and cobalt ions when cut (red) and after further addition of **2** (blue). The connection yield for this three-step strategy was roughly 9% (9 out of 103 devices tested). The different connection yields obtained through the two- and three-step processes may reflect the statistical distribution of the size of indented nanogaps formed by the dash-line cutting process. In these experiments we synthesized complex molecular wires in situ to bridge nanoscale electrodes through multistep reactions within nanogaps, which is rare in the field.

In summary, we have demonstrated the capability of installing molecular functionalities into electronic devices in a new platform of DLL-generated graphene–molecule junctions. We compared the device conductance and achieved reversible switching between distinct conductance states when devices with an azobenzene linker were either illuminated by light with different wavelengths or exposed to different pH values, thus indicating the possibility of integrating multiple functionalities into a single molecular device. In addition to building functional molecular circuits, we also demonstrated a useful method for the in situ construction of molecular transport junctions through the implementation of a programmed reaction sequence without the use of dithiolated molecules. This should overcome the problems associated with molecular oxidation and aggregation. We expect that these methods of creating nanoscale circuits and installing molecular functionalities by utilizing different functional building blocks will be useful for the development of new types of molecular electronic devices with diverse functions toward practical applications.

Received: October 12, 2012
Published online: March 4, 2013

Keywords: graphene · molecular devices · switching

[1] a) S. M. Lindsay, M. A. Ratner, *Adv. Mater.* **2007**, *19*, 23–31; b) N. J. Tao, *Nat. Nanotechnol.* **2006**, *1*, 173–181; c) M. Galperin, M. A. Ratner, A. Nitzan, A. Troisi, *Science* **2008**, *319*, 1056–1060; d) A. K. Feldman, M. L. Steigerwald, X. Guo, C. Nuckolls, *Acc. Chem. Res.* **2008**, *41*, 1731–1741; e) R. L. McCreery, A. J. Bergren, *Adv. Mater.* **2009**, *21*, 4303–4322; f) T. Li, W. Hu, D. Zhu, *Adv. Mater.* **2010**, *22*, 286–300; g) H. Song, M. A. Reed, T. Lee, *Adv. Mater.* **2011**, *23*, 1583–1608.

[2] a) S. Kubatkin, A. Danilov, M. Hjort, J. Cornil, J.-L. Brédas, N. Stuhr-Hansen, P. Hedegård, T. Bjørnholm, *Nature* **2003**, *425*, 698–701; b) N. B. Zhitenev, H. Meng, Z. Bao, *Phys. Rev. Lett.* **2002**, *88*, 226801–226804; c) M. A. Reed, C. Zhou, C. J. Muller, T. P. Burgin, J. M. Tour, *Science* **1997**, *278*, 252–254; d) Z. J. Donhauser, B. A. Mantooth, K. F. Kelly, L. A. Bumm, J. D. Monnell, J. J. Stapleton, D. W. Price, Jr., A. M. Rawlett, D. L. Allara, J. M. Tour, P. S. Weiss, *Science* **2001**, *292*, 2303–2307; e) B. Xu, N. J. Tao, *Science* **2003**, *301*, 1221–1223; f) X. D. Cui, A. Primak, X. Zarate, J. Tomfohr, O. F. Sankey, A. L. Moore, T. A. Moore, D. Gust, G. Harris, S. M. Lindsay, *Science* **2001**, *294*, 571–574; g) W. P. Hu, H. Nakashima, K. Furukawa, Y. Kashimura, K. Ajito, Y. Q. Liu, D. B. Zhu, K. Torimitsu, *J. Am. Chem. Soc.* **2005**, *127*, 2804–2805; h) L. Qin, S. Park, L. Huang, C. A.

Mirkin, *Science* **2005**, *309*, 113 – 115; i) X. Guo, J. P. Small, J. E. Klare, Y. Wang, M. S. Purewal, I. W. Tam, B. H. Hong, R. Caldwell, L. Huang, S. O'Brien, J. Yan, R. Breslow, S. J. Wind, J. Hone, P. Kim, C. Nuckolls, *Science* **2006**, *311*, 356 – 359; j) J. Park, A. N. Pasupathy, J. I. Goldsmith, C. Chang, Y. Yaish, J. R. Petta, M. Rinkoski, J. P. Sethna, H. D. Abruña, P. L. McEuen, D. C. Ralph, *Nature* **2002**, *417*, 722 – 725.

[3] a) J. Chen, M. A. Reed, A. M. Rawlett, J. M. Tour, *Science* **1999**, *286*, 1550 – 1552; b) R. E. Holmlin, R. Haag, M. L. Chabinyc, R. F. Ismagilov, A. E. Cohen, A. Terfort, M. A. Rampi, G. M. Whitesides, *J. Am. Chem. Soc.* **2001**, *123*, 5075 – 5085; c) J. G. Kushmerick, D. B. Holt, S. K. Pollack, M. A. Ratner, J. C. Yang, T. L. Schull, J. Naciri, M. H. Moore, R. Shashidhar, *J. Am. Chem. Soc.* **2002**, *124*, 10654 – 10655; d) H. B. Akkerman, P. W. M. Blom, D. M. de Leeuw, B. de Boer, *Nature* **2006**, *441*, 69 – 72; e) J. K. N. Mbindyo, T. E. Mallouk, J. B. Mattzela, I. Kratochvilova, B. Razavi, T. N. Jackson, T. S. Mayer, *J. Am. Chem. Soc.* **2002**, *124*, 4020 – 4026.

[4] a) R. M. Metzger, *Chem. Rev.* **2003**, *103*, 3803 – 3834; b) Y. Cao, M. L. Steigerwald, C. Nuckolls, X. Guo, *Adv. Mater.* **2010**, *22*, 20 – 32; c) C. W. Marquardt, S. Grunder, A. Błaszczyk, S. Dehm, F. Hennrich, H. von Löhneysen, M. Mayor, R. Krupke, *Nat. Nanotechnol.* **2010**, *5*, 863 – 867; d) H. Zhu, T. Li, Y. Zhang, H. Dong, J. Song, H. Zhao, Z. Wei, W. Xu, W. Hu, Z. Bo, *Adv. Mater.* **2010**, *22*, 1645 – 1648; e) S. Liu, Z. Wei, Y. Cao, L. Gan, Z. Wang, W. Xu, X. Guo, D. Zhu, *Chem. Sci.* **2011**, *2*, 796 – 802; f) X. Guo, S. Xiao, M. Myers, Q. Miao, M. L. Steigerwald, C. Nuckolls, *Proc. Natl. Acad. Sci. USA* **2009**, *106*, 691 – 696; g) Y. Cao, Z. Wei, S. Liu, Q. Shen, L. Gan, S. Shi, X. Guo, W. Xu, M. L. Steigerwald, Z. Liu, D. Zhu, *Angew. Chem.* **2010**, *122*, 6463 – 6467; *Angew. Chem. Int. Ed.* **2010**, *49*, 6319 – 6323.

[5] a) S. Liu, X. Guo, *NPG Asia Mater.* **2012**, *4*, e23; DOI: 10.1038/am.2012.42; b) S. Liu, X. Y. Zhang, W. X. Luo, Z. X. Wang, X. Guo, M. L. Steigerwald, X. H. Fang, *Angew. Chem.* **2011**, *123*, 2544 – 2550; *Angew. Chem. Int. Ed.* **2011**, *50*, 2496 – 2502; c) S. Liu, G. H. Clever, Y. Takezawa, M. Kaneko, K. Tanaka, X. Guo, M. Shionoya, *Angew. Chem.* **2011**, *123*, 9048 – 9052; *Angew. Chem. Int. Ed.* **2011**, *50*, 8886 – 8890; d) H. Wang, N. B. Muren, D. Ordinario, A. A. Gorodetsky, J. K. Barton, C. Nuckolls, *Chem. Sci.* **2012**, *3*, 62 – 65.

[6] a) D. Dulic, S. J. van der Molen, T. Kudernac, H. T. Jonkman, J. J. D. de Jong, T. N. Bowden, J. van Esch, B. L. Feringa, B. J. van Wees, *Phys. Rev. Lett.* **2003**, *91*, 207402; b) S. J. van der Molen, H. van der Vegte, T. Kudernac, I. Amin, B. L. Feringa, B. J. van Wees, *Nanotechnology* **2006**, *17*, 310 – 314; c) J. He, F. Chen, P. A. Liddell, J. Andréasson, S. D. Straight, D. Gust, T. A. Moore, A. L. Moore, J. Li, O. F. Sankey, S. M. Lindsay, *Nanotechnology* **2005**, *16*, 695 – 702; d) N. Katsonis, T. Kudernac, M. Walko, S. J. van der Molen, B. J. van Wees, B. L. Feringa, *Adv. Mater.* **2006**, *18*, 1397 – 1400; e) A. C. Whalley, M. L. Steigerwald, X. Guo, C. Nuckolls, *J. Am. Chem. Soc.* **2007**, *129*, 12590 – 12591.

[7] a) J. M. Tour, L. Jones II, D. L. Pearson, J. J. S. Lamba, T. P. Burgin, G. M. Whitesides, D. L. Allara, A. N. Parikh, S. Atre, *J. Am. Chem. Soc.* **1995**, *117*, 9529 – 9534; b) M. Taniguchi, Y. Nojima, K. Yokota, J. Terao, K. Sato, N. Kambe, T. Kawai, *J. Am. Chem. Soc.* **2006**, *128*, 15062 – 15063.

[8] a) J. Y. Tang, Y. L. Wang, J. E. Klare, G. S. Tulevski, S. J. Wind, C. Nuckolls, *Angew. Chem.* **2007**, *119*, 3966 – 3969; *Angew. Chem. Int. Ed.* **2007**, *46*, 3892 – 3895; b) X. Chen, A. B. Braunschweig, M. J. Wiester, S. Yeganeh, M. A. Ratner, C. A. Mirkin, *Angew. Chem.* **2009**, *121*, 5280 – 5283; *Angew. Chem. Int. Ed.* **2009**, *48*, 5178 – 5181.

[9] a) *Molecular switches* (Ed.: B. Feringa), Wiley-VCH, Weinheim, **2001**; b) A. A. Beharry, G. A. Woolley, *Chem. Soc. Rev.* **2011**, *40*, 4422 – 4437.

[10] a) M. del Valle, R. Gutierrez, C. Tejedor, G. Cuniberti, *Nat. Nanotechnol.* **2007**, *2*, 176 – 179; b) C. Zhang, M.-H. Du, H.-P. Cheng, X.-G. Zhang, A. E. Roitberg, J. L. Krause, *Phys. Rev. Lett.* **2004**, *92*, 158301; c) C. Zhang, Y. He, H.-P. Cheng, *Phys. Rev. B* **2006**, *73*, 125445.

[11] a) B.-Y. Choi, S.-J. Kahng, S. Kim, H. Kim, H. W. Kim, Y. J. Song, J. Ihm, Y. Kuk, *Phys. Rev. Lett.* **2006**, *96*, 156106; b) S. Loudwig, H. Bayley, *J. Am. Chem. Soc.* **2006**, *128*, 12404 – 102405; c) P. Paoprasert, B. Park, H. Kim, P. Colavita, R. J. Hamers, P. G. Evans, P. Gopalan, *Adv. Mater.* **2008**, *20*, 4180 – 4184; d) A. S. Kumar, T. Ye, T. Takami, B.-C. Yu, A. K. Flatt, J. M. Tour, P. S. Weiss, *Nano Lett.* **2008**, *8*, 1644 – 1648; e) J. Iwicki, E. Ludwig, M. Kalläne, J. Buck, F. Köhler, R. Herges, L. Kipp, K. Rossnagel, *Appl. Phys. Lett.* **2010**, *97*, 063112; f) M. Kim, N. S. Safron, C. Huang, M. S. Arnold, P. Gopalan, *Nano Lett.* **2012**, *12*, 182 – 187.

[12] Y. Cao, S. Dong, S. Liu, L. He, L. Gan, X. Yu, M. L. Steigerwald, X. Wu, Z. Liu, X. Guo, *Angew. Chem.* **2012**, *124*, 12394 – 12398; *Angew. Chem. Int. Ed.* **2012**, *51*, 12228 – 12232.

[13] a) J.-C. Chiang, A. G. MacDiarmid, *Synth. Met.* **1986**, *13*, 193 – 194; b) X. Guo, D. Zhang, G. Yu, M. Wan, J. Li, Y. Liu, D. Zhu, *Adv. Mater.* **2004**, *16*, 636 – 640.